Extended MHD solutions for plasma-vacuum interface that is singularly perturbed by electron inertia

Makoto Hirota
Institute of Fluid Science,
Tohoku University

1 Introduction

Magnetohydrodynamics (MHD) is an approximate model that describes large-scale behavior of dense plasma. The standard MHD equations are derived by neglecting gyro-radii and inertial lengths for both ions and electrons, since these scales are often small in comparison to the length scale of dynamics that we are interested in. However, this MHD approximation is well known to be invalid when the mass density (ρ) tends to zero. In fact, the phase speed of the Alfvén wave, which is given by $v_A = B/\sqrt{\mu_0 \rho}$ in MHD, diverges unphysically when $\rho \to 0$, which makes numerical simulation unstable. Therefore, MHD can not correctly deal with interface between plasma and vacuum regions (namely, the free-boundary problem). This drawback limits the application of MHD, since plasmas are often surrounded by nearly vacuum region (such as space plasmas around celestial bodies and magnetically confined plasmas in fusion experimental devices).

In MHD, Ohm's law is written as

$$\boldsymbol{E} + \boldsymbol{v} \times \boldsymbol{B} = \eta \boldsymbol{J}, \tag{1}$$

where $\boldsymbol{E}$ is electric field, $\boldsymbol{v}$ is velocity field, $\boldsymbol{B}$ is magnetic field, η is resistivity, $\boldsymbol{J}$ is current density. In experiments, the electric field is usually applied by external coils to generate discharge plasma in vacuum vessel. When η is a finite value, a nonzero current $\boldsymbol{J}$ is driven by $\boldsymbol{E}$ even in the vacuum region. To suppress this unphysical current in vacuum, we need to make resistivity diverge; $\eta(\rho) \to \infty$ as $\rho \to 0$. In practice, a sufficiently large resistivity is used for numerical simulation, which is called the pseudo-vacuum model. Such the extremely fast magnetic diffusion (and fast Alfvén speed as well) necessitates the use of implicit numerical scheme for time marching. The computational cost, therefore, increases significantly in the presence of nearly vacuum region, in which the validity of the MHD approximation is still questionable.

Now, it should be remembered that both the ion's and electron's inertial lengths (d_i, d_e) are inversely proportional to $\sqrt{\rho}$. These scales introduce the so-called two-fluid effect, which is neglected in MHD, but they are obviously no longer small scales when the density approaches to zero. If one do not neglect the ion inertial length d_e, the Hall effect newly appears in MHD (called Hall MHD). In addition, if one do not neglect the electron inertial length d_e, the electron-inertia effect appears. The governing system is called the extended MHD (XMHD, in short) [1] if both d_i and d_e are included (which is almost equivalent to the two-fluid model but only the charge neutrality condition is imposed). Above all, the electron inertia drastically modifies the property of MHD in vacuum. In fact, in the limit of vacuum $\rho \to 0$, the Alfvén speed becomes finite [2] and the current becomes zero *because of the electron inertia*. It should be emphasized that this is the physically true behavior of plasma that the MHD approximation overlooks.

The XMHD equations are shown to be a Hamiltonian system [3, 4] and several conservation laws are clarified [5]. However, the actual solution of XMHD is not so extensively studied in literature. In this paper, we consider the simplest equilibrium state in cylindrical geometry, which is called Z-pinch equilibrium in the community of magnetically confined plasma. In this equilibrium state, cylindrical plasma is confined by a radial $\boldsymbol{J} \times \boldsymbol{B}$ pinch force and, hence, the pressure (and density) decays radially and becomes vacuum at a certain position. By solving XMHD for this simple problem, this paper investigates how the plasma-vacuum interface is formed in XMHD and is affected by the electron inertia and viscosity.

2 The XMHD equations

Using representative scales of length (L), density and magnetic field, we normalize the XMHD equations, where velocity is normalized by the Alfvén speed. The governing equations [1, 6] are then written as

$$\frac{\partial \rho}{\partial t} + \nabla \cdot (\rho \boldsymbol{v}) = 0, \tag{2}$$

$$\rho \left(\frac{\partial \boldsymbol{v}}{\partial t} + \boldsymbol{v} \cdot \nabla \boldsymbol{v} \right) = -\nabla p + \boldsymbol{J} \times \boldsymbol{B} - \epsilon_I^2 \boldsymbol{J} \cdot \nabla \left(\frac{\boldsymbol{J}}{\rho} \right) - \frac{1}{\tau_n} \rho \boldsymbol{v} + \Delta_{\mathrm{vis}}(\mu, \boldsymbol{v}), \tag{3}$$

$$\begin{aligned} \boldsymbol{E} + \boldsymbol{v} \times \boldsymbol{B} - \frac{\epsilon_H}{\rho} (\boldsymbol{J} \times \boldsymbol{B} - \nabla p_H) =& \frac{\epsilon_I^2}{\rho} \left[\frac{\partial \boldsymbol{J}}{\partial t} + \nabla \cdot \left(\boldsymbol{v}\boldsymbol{J} + \boldsymbol{J}\boldsymbol{v} - \frac{\epsilon_H}{\rho} \boldsymbol{J}\boldsymbol{J} \right) \right] \\ &+ \eta \boldsymbol{J} + \frac{\epsilon_I^2}{\tau_n} \frac{\boldsymbol{J}}{\rho} - \frac{\epsilon_I^2}{\rho} \Delta_{\mathrm{vis}} \left(\mu, \frac{\boldsymbol{J}}{\rho} \right), \end{aligned} \tag{4}$$

$$\frac{\partial \boldsymbol{B}}{\partial t} = -\nabla \times \boldsymbol{E}, \tag{5}$$

$$\boldsymbol{J} = \nabla \times \boldsymbol{B}, \tag{6}$$

where

$$\epsilon_I := \frac{d_e}{L\sqrt{1+\epsilon}}, \quad \epsilon_H := \frac{d_i(1-\epsilon)}{L\sqrt{1+\epsilon}}, \tag{7}$$

are the nondimensional parameters manifesting the electron-inertia and Hall effects, respectively ($\epsilon = m_e/m_i$ is the mass ratio between electron and ion, which is usually neglected). The simple collisional effects are introduced as the dissipation terms in the above equations; $1/\tau_n$ represents the decay time due to collision with background neutral particles. The viscosity term is taken to be

$$[\Delta_{\mathrm{vis}}(\mu, \boldsymbol{v})]_j = \frac{\partial}{\partial x_i} \left[\mu \left(\frac{\partial v_i}{\partial x_j} + \frac{\partial v_j}{\partial x_i} - \frac{2}{3} \delta_{ij} \nabla \cdot \boldsymbol{v} \right) \right], \tag{8}$$

where μ is the viscosity coefficient. Finally, we assume that both ions and electrons are barotropic fluids for simplicity, so $p(\rho)$ and $p_H(\rho)$ are functions of ρ.

To solve the XMHD equations, we should eliminate $\boldsymbol{E}$. Alternatively, it is more beneficial to introduce the vector and scalar potentials; $\boldsymbol{E} = -\partial \boldsymbol{A}/\partial t - \nabla \phi$ and $\boldsymbol{B} = \nabla \times \boldsymbol{A}$. The governing equations are rewritten as

$$\frac{\partial \rho}{\partial t} = -\nabla \cdot (\rho \boldsymbol{v}), \tag{9}$$

$$\frac{\partial \boldsymbol{v}}{\partial t} = \boldsymbol{v} \times (\nabla \times \boldsymbol{v}) + \frac{\boldsymbol{J}}{\rho} \times \boldsymbol{B}^\star - \nabla \left(\frac{|\boldsymbol{v}|^2}{2} + h(\rho) + \epsilon_I^2 \frac{|\boldsymbol{J}|^2}{2\rho^2} \right) - \frac{1}{\tau_n} \boldsymbol{v} + \frac{1}{\rho} \Delta_{\mathrm{vis}}(\mu, \boldsymbol{v}), \tag{10}$$

$$\frac{\partial \boldsymbol{A}^\star}{\partial t} = \left(\boldsymbol{v} - \epsilon_H \frac{\boldsymbol{J}}{\rho} \right) \times \boldsymbol{B}^\star + \epsilon_I^2 \frac{\boldsymbol{J}}{\rho} \times (\nabla \times \boldsymbol{v}) + \nabla(\dots) - \left(\eta + \frac{\epsilon_I^2}{\tau_n} \frac{1}{\rho} \right) \boldsymbol{J} + \frac{\epsilon_I^2}{\rho} \Delta_{\mathrm{vis}} \left(\mu, \frac{\boldsymbol{J}}{\rho} \right), \tag{11}$$

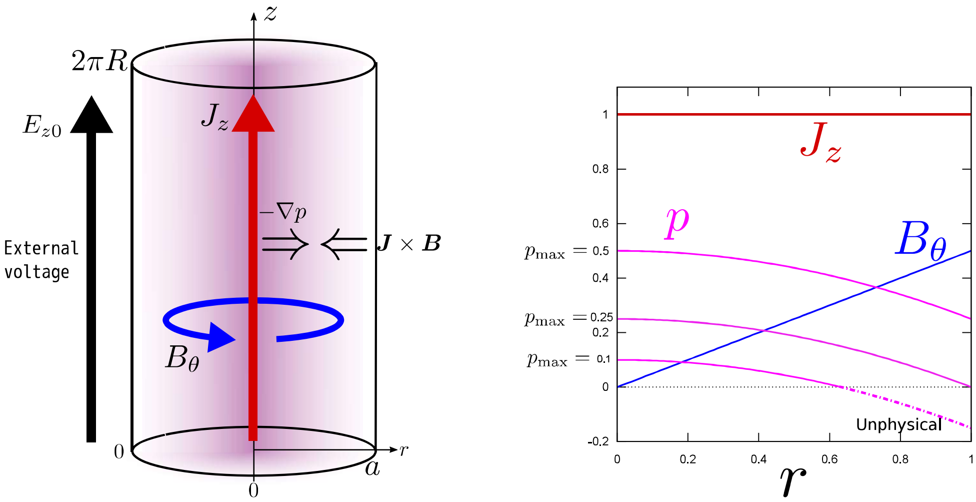

Fig.1 Z-pinch equilibrium in cylindrical geometry

where $h(\rho)$ is the enthalpy defined by $\nabla h(\rho) = \rho^{-1}\nabla p(\rho)$, and

$$\boldsymbol{A}^\star := \boldsymbol{A} + \epsilon_I^2 \frac{\boldsymbol{J}}{\rho}, \quad \boldsymbol{B}^\star := \nabla\times\boldsymbol{A}^\star = \boldsymbol{B} + \epsilon_I^2 \nabla\times\frac{\boldsymbol{J}}{\rho}. \tag{12}$$

It should be remarked that $\boldsymbol{u} = \boldsymbol{J}/\rho = \boldsymbol{v}_i - \boldsymbol{v}_e$ represents the relative velocity field between ion and electron, which is now expressed as $\boldsymbol{u} = \rho^{-1}\nabla\times(\nabla\times\boldsymbol{A})$. Because of the arbitrariness of gauge, the gradient terms $\nabla(\dots)$, which include ϕ, are unimportant and have nothing to do with the actual dynamics.

Thus, the XMHD equations constitute a dynamical system of $(\rho, \boldsymbol{v}, \boldsymbol{A}^\star)$. The number of field variables is the same as MHD, but one has to obtain $\boldsymbol{A}$ by solving

$$\boldsymbol{A}^\star = \boldsymbol{A} + \frac{\epsilon_I^2}{\rho}\nabla\times(\nabla\times\boldsymbol{A}), \tag{13}$$

with an appropriate boundary condition. The numerical cost is increased by this additional procedure, which stems from the constraint of quasi-neutrality $\nabla[\rho(\boldsymbol{v}_i - \boldsymbol{v}_e)] = 0$. As a similar problem, recall that, in fluid mechanics, one has to solve the Poisson equation additionally when the constraint of incompressibility $\nabla\cdot\boldsymbol{v} = 0$ is imposed. The equation (13) manifests a very important role of electron inertia $\epsilon_I^2 \neq 0$. Even if ϵ_I^2 is a small parameter, this term is not negligible when the density ρ becomes as low as ϵ_I^2. In fact, the solution of (13) corresponds to vacuum magnetic field $\nabla\times(\nabla\times\boldsymbol{A}) \to 0$ as $\rho \to 0$. Moreover, because of this electron-inertia effect, the Alfvén speed $v_A = B/\sqrt{\rho}$ in MHD is modified to $v_A^\star = B/\sqrt{\rho + \epsilon_I^2 k^2}$ in XMHD, where k is the wavenumber of Alfvén wave. Therefore, the Alfvén speed does not diverge unphysically even at vacuum region $\rho \to 0$. Solving (13) is costly, but all unphysical properties of MHD in vacuum is amended by it. The electron-inertia effect is clearly a singular perturbation to MHD; it shows up either in small scale $k \sim 1/\epsilon_I$ or in low density $\rho \sim \epsilon_I^2$.

3 Z-pinch equilibrium

By solving the XMHD equations, it is expected that we obtain appropriate solutions including low-density or vacuum region. Let us consider the Z-pinch equilibrium state as an example to demonstrate it. In the cylindrical geometry (r, θ, z) shown in Fig. 1, a constant electric field $E_{z0} =$ const. is applied in z direction by some external coil. In MHD, a steady equilibrium solution is obtained by solving

$$-\nabla p + \boldsymbol{J} \times \boldsymbol{B} = 0, \tag{14}$$

$$\boldsymbol{E} = \eta \boldsymbol{J}. \tag{15}$$

If resistivity η is constant, the solution is

$$J_z = \frac{E_{z0}}{\eta}, \quad B_\theta = \frac{E_{z0}}{2\eta} r, \quad p = p_{\max} - \frac{E_{z0}^2}{4\eta^2} r^2, \tag{16}$$

where $p_{\max}$ is an arbitrary parameter. When the maximum pressure $p_{\max}$ is relatively small, we can easily find that pressure becomes zero at a certain radius as shown in Fig. 1. Throughout this paper, the equation of state is assumed to be

$$p(\rho) = \frac{c_{s0}^2}{\gamma} \rho^\gamma, \tag{17}$$

where γ is the specific heat ratio and c_{s0} is the sound speed at $\rho = 1$. In the case of adiabatic change, $\gamma = 5/3$ is often chosen. On the other hand, $\gamma = 1$ corresponds to isothermal change of ideal gas. In any case, $p = 0$ corresponds to $\rho = 0$, which indicates the position of plasma-vacuum interface. However, since J_z flows constantly also in vacuum region, this MHD solution needs to be amended.

One remedy is to take the collision with neutral particles into account in Ohm's law,

$$\boldsymbol{E} = \left(\eta + \frac{\epsilon_I^2}{\tau_n \rho} \right) \boldsymbol{J} \quad \Rightarrow \quad J_z = \frac{\rho}{\rho + \epsilon_I^2/(\tau_n \eta)} \frac{E_{z0}}{\eta}. \tag{18}$$

The resistivity is effectively replaced by $\eta + \epsilon_I^2/(\tau_n \rho)$ which diverges in vacuum. Then, the current J_z becomes zero smoothly as $\rho \to 0$. An example of solution is shown in Fig. 2 for the case of $\gamma = 5/3$, $\beta = c_{s0}^2 \eta^2/(\gamma E_{z0}^2) = 0.018$ and $\epsilon_I^2/(\tau_n \eta) = 0.001$, where we can set $r = 1$ as the wall position and $E_{z0}/\eta = 1$ by choosing the normalization appropriately. Here, the parameter β represents the ratio of plasma pressure to magnetic pressure. At the position where the density reaches zero, the current sharply drops to zero [because $\epsilon_I^2/(\tau_n \eta)$ is small] and vacuum region appears outside it. This is essentially equivalent to what we do in the pseudo-vacuum model (i.e., very large resistivity is introduced in vacuum).

Another remedy is to solve the XMHD equations by taking the electron-inertia into account. In this paper, let us mainly consider this remedy instead of using the psuedo-vacuum model. In XMHD, it is interesting to note that the vacuum region is filled with "ghost plasma" in a sense. The velocity $\boldsymbol{v}$ and relative velocity $\boldsymbol{u}$ are generally not zero in the vacuum region, but the mass flow and electric current are zero, $\rho \boldsymbol{v} = 0$ and $\boldsymbol{J} = \rho \boldsymbol{u} = 0$, just because $\rho = 0$ in vacuum. By assuming that the steady solution depends on only the radial coordinate r, the XMHD equations are reduced to a system of first order ordinary differential equations (ODEs) for 4 variables $(\rho, u_z, u_z', B_\theta)$ (where $' := d/dr$),

$$\rho' = -\frac{\rho^{2-\gamma}}{c_{s0}^2} B_\theta u_z, \tag{19}$$

$$\frac{\epsilon_I^2}{\rho r} (r \mu u_z')' = \eta \rho u_z - E_{z0}, \tag{20}$$

$$\frac{1}{r} (r B_\theta)' = \rho u_z, \tag{21}$$

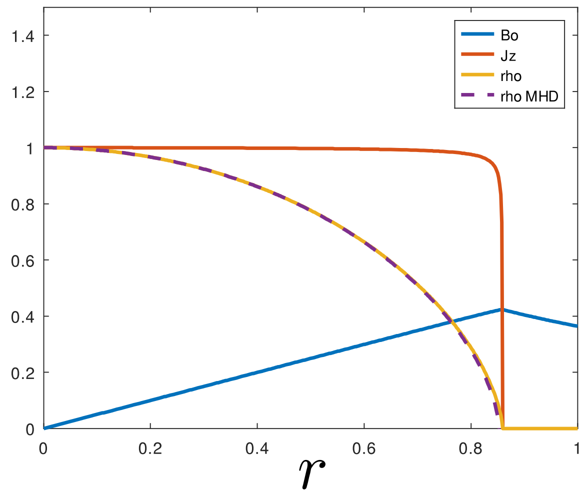

Fig.2 MHD solution with the pseudo-vacuum model $\epsilon_I^2/\tau_n = 0.001$, where $\gamma = 5/3$ and $\beta = 0.018$.

with $J_z = \rho u_z$. The terms with ϵ_H are included into the gradient fields and, hence, the Hall effect does not essentially affect the steady solution. The terms with ϵ_I also vanish mostly at the steady state. Only the viscosity term remains in Ohm's law (20) as the remnant of considering electron inertia. Since the solution must be regular at $r = 0$, the regularity condition is given by

$$\rho = 1 + O(r^2), \tag{22}$$

$$u_z' = \frac{1}{2\epsilon_I^2 \mu(0)} \left(\eta u_z(0) - E_{z0}\right) r + O(r^3), \tag{23}$$

$$u_z = u_z(0) + O(r^2), \tag{24}$$

$$B_\theta = u_z(0)\frac{r}{2} + O(r^3), \tag{25}$$

where $u_z(0)$ is arbitrary. On the other hand, it is natural to impose the no-slip boundary condition $u_z(1) = 0$ at the wall $r = 1$. Therefore, we can solve the system of ODEs numerically by the shooting method, where $u_z(0)$ is adjusted such that $u_z(1) = 0$ holds.

4 Singularity at plasma-vacuum interface

The system of ODEs (19)-(21) is strongly nonlinear. Since the viscosity exists, suppose that $u_z(r)$ is a continuous function and takes a nonzero value at the plasma-vacuum interface. The same is supposed for B_θ since it is obtained by integrating (21). Then, $B_\theta u_z$ in (19) is approximated by a constant in the neighborhood of the interface, which corresponds to the inward pinch force. Based on this observation, let us consider the following toy problem.

$$\rho' = -2\rho^{2-\gamma} r, \quad \rho(0) = 1. \tag{26}$$

The solution is easily obtained as

$$\rho = \begin{cases} \left[1 - (\gamma - 1)r^2\right]^{\frac{1}{\gamma-1}} & \gamma \neq 1 \\ e^{-r^2} & \gamma = 1 \end{cases}. \tag{27}$$

When $\gamma = 1$ (isothermal change), the density ρ decays exponentially outward, which is smooth and never reaches zero. We cannot define the rigorous position of the plasma-vacuum interface in

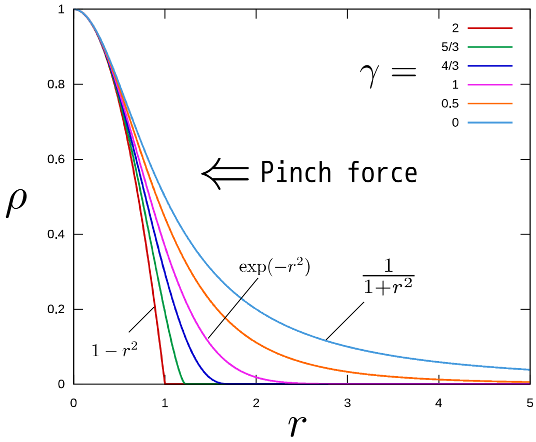

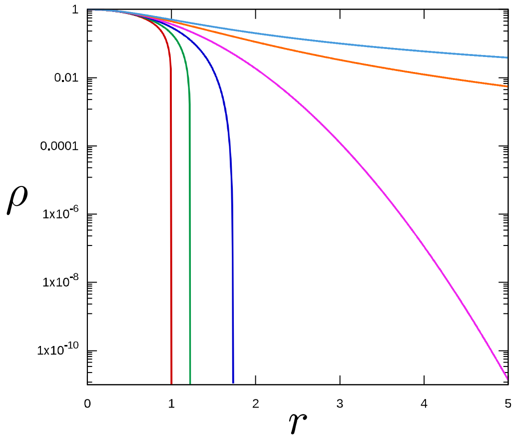

Fig.3 The solutions (27) of the toy problem (26). The right figure is the semi-log plot.

this case (similar to the atmospheric stratification on the earth). However, when $\gamma > 1$ (adiabatic change), the density ρ becomes zero at a position, say, $r = a$, which is exactly the plasma-vacuum interface. On the vacuum side $r > a$, the trivial solution $\rho = 0$ of (26) exists. In the neighborhood of $r = a$ on the plasma side $r < a$, the solution behaves singularly like $\rho \propto (a-r)^{1/(\gamma-1)}$. Therefore, the shooting method fails at plasma-vacuum interface when the adiabatic change $\gamma > 1$ is assumed.

As an numerical technique, we can regularize this singularity at $r = a$ as follows. First, we solve $\log \rho$ instead of ρ such that ρ does not become negative due to numerical error. Next, (19) is slightly modified into

$$(\log \rho)' = -\frac{(\rho + 10^{-6})^{1-\gamma}}{c_{s0}^2} B_\theta u_z, \tag{28}$$

where a tiny number 10^{-6} is inserted as an example. Only when ρ gets lower than 10^{-6}, this modification comes into effect, that is, ρ decays like exponential function since the right hand side does not become zero. In other words, $\gamma > 1$ is modified to $\gamma = 1$ only when $\rho < 10^{-6}$. Using this regularization technique, the shooting method works correctly. Although extremely low density $\rho < 10^{-6}$ exists in the vacuum region, it can be regarded as numerical error.

5 Role of viscosity in equilibrium solution

The viscosity plays a decisive role in determining the Z-pinch equilibrium of XMHD. As an *inappropriate* example, let us consider

$$-\epsilon_I^2 \nu \frac{1}{r}(r u_z')' + \eta_0 \rho u_z = E_{z0}, \tag{29}$$

in place of (20). This viscosity term is equivalent to the Laplacian term $\nu \Delta \boldsymbol{u}$ that appears in the Navier-Stokes equation for *incompressible* fluid. This form of viscosity is often adopted for compressible MHD simulation, because it is easy to implement and works well as an energy sink that suppress numerical instability.

In this case, several solutions are displayed in Fig. 4. In comparison to the MHD solution indicated by the dashed line, the density tends to decrease more steeply and becomes zero at a smaller radius. The limit of $\epsilon_I^2\nu/\eta \to 0$ is supposed to match the MHD solution, but the result is in fact the contrary. We can observe that the current J_z tends to be concentrated on the plasma surface in this limit, which implies a formation of boundary layer. It is also remarkable that u_z gets larger in vacuum region in Fig. 4. When $\rho = 0$, the relative velocity u_z is accelerated by E_{z0} until the viscosity balances. For example, if the density ρ were zero everywhere, the solution of (29) would be

$$u_z = \frac{E_{z0}}{4\epsilon_I^2\nu}(1 - r^2), \tag{30}$$

which is understood as the Poiseuille flow driven by a constant force E_{z0}. The smaller the viscosity, the faster the flow. In this way, there exists ghost plasma and we solve the velocity field u_z even in vacuum. Multiplication of this large u_z and the density profile ρ results in the current layer $J_z = \rho u_z$ at the plasma surface.

By assuming the existence of a boundary layer in the MHD limit $\epsilon_I^2\nu/\eta \to 0$, the XMHD solution in Fig. 4 can be predicted analytically as follows. Let $r = a$ be the position where ρ becomes exactly zero, and $a - \delta < r < a$ be a boundary layer. The thickness δ of the layer is assumed to be

$$\delta \to 0 \quad \text{as} \quad \epsilon_* := \epsilon_I^2\nu/\eta \to 0.$$

In the inner region $0 \le r < a - \delta$, we can expect the MHD solution (16),

$$\rho = \left(1 - \frac{r^2}{4\beta_*}\right)^{\frac{1}{\gamma}}, \tag{31}$$

$$u_z = \left(1 - \frac{r^2}{4\beta_*}\right)^{-\frac{1}{\gamma}}, \tag{32}$$

$$B_\theta = \frac{r}{2}, \tag{33}$$

where $\beta_* := c_{s0}^2\eta^2/(\gamma E_{z0}^2)$. In the outer region $a < r < 1$, the vacuum solution is given by

$$\rho = 0, \tag{34}$$

$$u_z = \frac{1 - r^2}{4\epsilon_*} + \frac{aB_\theta(a)}{\epsilon_*}\log r, \tag{35}$$

$$B_\theta = \epsilon_* u_z' + \frac{r}{2} = \frac{a}{r}B_\theta(a), \tag{36}$$

which satisfies the boundary condition $u_z = 0$ at $r = 1$. However, the two parameters, a and $B_\theta(a)$, are still unknown. They can be determined by the matching conditions between the inner and outer solutions. Suppose again that u_z is a continuous function,

$$u_z(a - \delta) \to u_z(a) \quad \text{as} \quad \delta \to 0, \tag{37}$$

In the momentum equation, the balance between pressure and $\boldsymbol{J} \times \boldsymbol{B}$ force is simply

$$p' = -\frac{(B_\theta^2)'}{2} - \frac{B_\theta^2}{2}, \tag{38}$$

where B_θ must be a continuous function (otherwise, the energy of the solution would diverge). By integrating this equation over the thin layer $[a - \delta, a]$, the so-called total pressure is also continuous as follows.

$$p(a - \delta) + \frac{B_\theta^2(a - \delta)}{2} \to p(a) + \frac{B_\theta^2(a)}{2} \quad \text{as} \quad \delta \to 0. \tag{39}$$

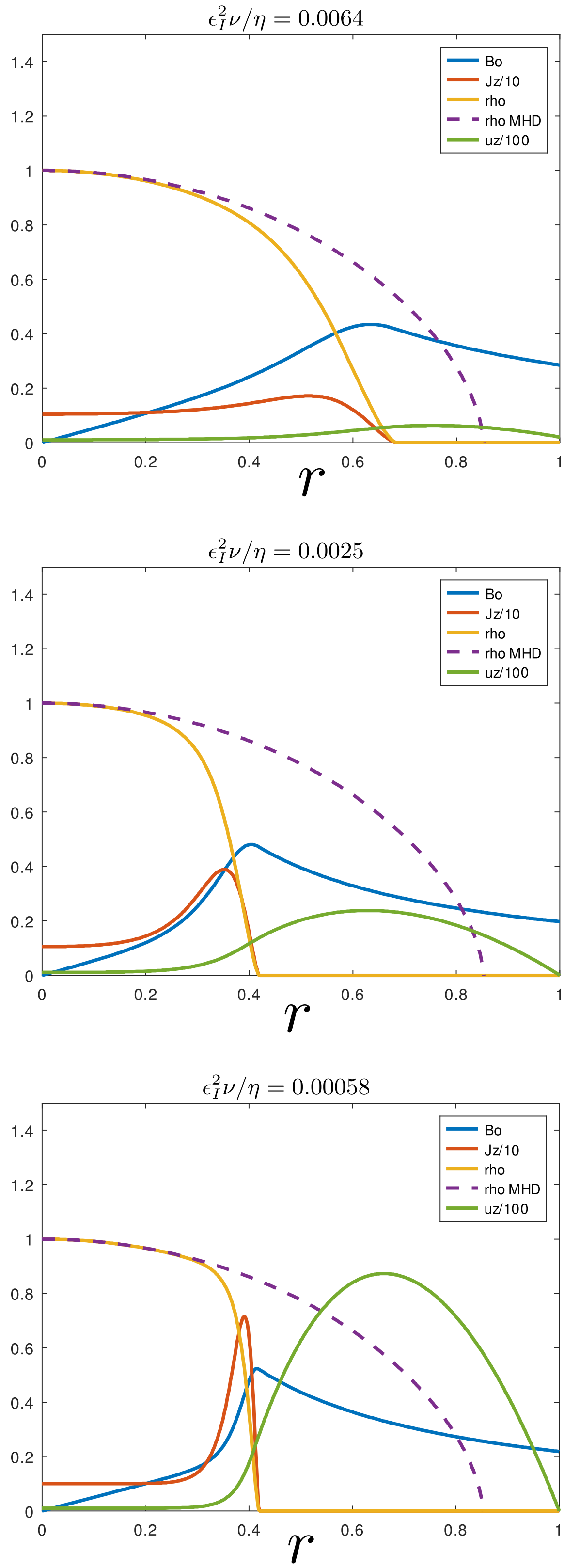

Fig.4 XMHD solution with the viscosity (29) where $\gamma = 5/3$, $\beta = 0.018$.

Using these two matching conditions (37) and (39), the two parameters a and $B_\theta(a)$ are determined as

$$\beta_* = \frac{a^2}{8} + \frac{1}{32}\left(\frac{1-a^2}{a\log a}\right)^2 =: f(a), \quad B_\theta(a) = -\frac{1-a^2}{4a\log a},$$

for given β_* in the limit of $\epsilon_* \to 0$. The function $\beta_* = f(a)$ is plotted in Fig. 5, where $f(0) = \infty$ and $f(1) = 1/4$. The position of plasma-vacuum interface a is determined by the reciprocal function $a = f^{-1}(\beta_*)$. Namely, there is no solution for $\beta_* < 0.1776$, whereas there are two solutions for $0.1776 < \beta_* < 0.25$. Since $B_\theta(a-0) = a/2$, there is a discontinuity $B_\theta(a-0) \neq B_\theta(a)$ as far as $a < 1$, which implies the existence of the surface current J_z like a delta function at the plasma-vacuum interface. The numerical solution indeed shows this tendency when ϵ_* is small.

It should be noted that, in the above solution, the density is normalized by its value at $r = 0$, so that the shooting method starts with $\rho(0) = 1$. Therefore, the total mass of the plasma

$$\langle\rho\rangle = \int_0^a \rho 2r dr = \frac{4\beta_*}{1/\gamma+1}\left[1 - \left(1 - \frac{a^2}{4\beta_*}\right)^{1/\gamma+1}\right] =: g(a, \beta_*), \tag{40}$$

varies depending on β_*. Given this result, let us modify the normalization of density to $\rho \to \rho/\langle\rho\rangle$. Then, other quantities are rescaled as follows.

$$u_z \to u_z\langle\rho\rangle, \quad \epsilon_* \to \epsilon_*/\langle\rho\rangle, \quad \beta_* \to \beta_*\langle\rho\rangle^\gamma. \tag{41}$$

Therefore, if the total mass is normalized to $\langle\rho\rangle = 1$, the relation between β_* and a is modified to

$$\beta_* = f(a)[g(a, f(a))]^\gamma. \tag{42}$$

This is found to be a monotonically increasing function of a, and $\beta_* = 0$ for $a = 0$. Therefore, there exists one solution for each β_*, which indicates that the plasma radius a shrinks as the plasma pressure β_* decreases.

6 Discussion

In this paper, we have demonstrated that the XMHD equations can deal with the plasma-vacuum interface. In vacuum region, we need to solve the velocity field of ghost plasma, imposing the proper boundary condition (such as the no-slip boundary condition in the presence of viscosity). Although the dynamics of ghost plasma is not important in reality, the formation of the surface current at the plasma-vacuum interface is related to the matching condition with the large velocity of ghost plasma. Unfortunately, this solution seems to be not physically appropriate and needs to be improved, because the viscous shear stress is large in the vacuum region. If we think of interfacial surface between water and air, the viscosity of air is much smaller than that of water, and hence the shear stress at the surface of water is almost zero. Namely, the free-boundary condition (or Neumann condition) approximately holds at the surface of water and the dynamics of air can be ignored. This treatment for air is analogous to ghost plasma. In XMHD, the viscosity is necessary for the existence of steady state under the electric field E_{z0}, but it should be very small in vacuum region to realize the bree-boundary.

Therefore, we should adopt the more realistic viscosity term (20) instead of (29), where the viscosity coefficient $\mu(\rho)$ should be a function of ρ which decreases as $\rho \to 0$. In fact, the steady

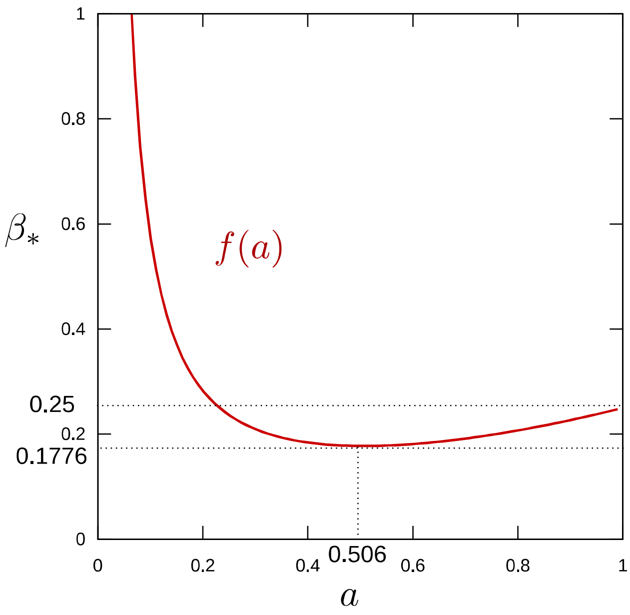

Fig.5 Plot of $\beta_* = f(a)$.

solution is significantly affected by the choice of $\mu(\rho)$. Further results on this nonconstant $\mu(\rho)$ will be reported elsewhere.

References

[1] K. Kimura and P. J. Morrison, Phys. Plasmas 21, 082101 (2014).

[2] B. Srinivasan and U. Shumlak, Phys. Plasmas, 18, 092113 (2011)

[3] M. Lingam, G. Miloshevich, and P. J. Morrison, Phys. Lett. A 380, 2400 (2016).

[4] E. C. D'Avignon, P. J. Morrison, and M. Lingam, Phys. Plasmas 23, 062101 (2016).

[5] H. M. Abdelhamid, Y. Kawazura, and Z. Yoshida, J. Phys. A: Math. Theor. 48, 235502 (2015).

[6] M. Hirota, Phys. Plasmas 28, 022106 (2021).

Institute of Fluid Science
Tohoku University
2-1-1, Katahira, Aoba-ku, Sendai, Miyagi, 980-8577
JAPAN
e-mail: makoto.hirota.d5@tohoku.ac.jp